

HEPATIC AND INTRAHEPATIC TARGETING OF AN ANTI-INFLAMMATORY AGENT WITH HUMAN SERUM ALBUMIN AND NEOGLYCOPROTEINS AS CARRIER MOLECULES

ERIC J. F. FRANSSEN,*† ROBERT W. JANSEN,‡ MARISKA VAALBURG‡ and
DIRK K. F. MEIJER‡

*University Hospital, Department of Nuclear Medicine, Division: PET-research Centre,
Oostersingel 59, 9713 EZ Groningen, and ‡University Center for Pharmacy,
Department of Pharmacology and Pharmacotherapy, Ant. Deusinglaan 2, 9713 AW Groningen,
The Netherlands

(Received 13 April 1992; accepted 18 December 1992)

Abstract—The anti-inflammatory agent naproxen (Nap) was covalently coupled to human serum albumin (HSA) and to the neoglycoproteins, galactose and mannose terminated HSA, to deliver this drug selectively to different cell types of the liver. Disposition of Nap₂₀-HSA was studied in rats and compared to that of equivalent doses of mixtures of uncoupled drug and protein. The liver to kidney ratios of the drug (L/K-Nap) and the protein (L/K-prot.) were increased, indicating an improved delivery of both protein and drug to the target site. After injection of 10 µg Nap₂₀-HSA the L/K-prot. was increased 15.0 ± 0.21-fold as measured 1 hr after injection. Even after injection of 5 mg of the conjugate, the L/K-prot. was enhanced 5.6 ± 0.34-fold and the L/K-Nap 4.6 ± 0.23-fold as measured 1 hr after injection. Immunohistochemical staining of liver slices revealed that the endothelial cells were the main sites for hepatic uptake. Further pharmacokinetic studies of Nap₂₀-HSA in isolated perfused rat livers showed a saturable uptake process ($V_{\max} = 2.46 \mu\text{g}/\text{min}/10.0 \text{ g liver}$ and $K_m = 4.27 \times 10^{-6} \text{ M}$). The uptake in the liver could be inhibited by various polyanionic probes, indicating the major involvement of a scavenger receptor system in the internalization mechanism of Nap₂₀-HSA. This endothelial uptake via the scavenger receptor system is likely to be related to the increased negative charge of the Nap-albumin conjugate as was revealed by anion exchange chromatography. Studies in the intact organ and in purified liver lysosomal lysates indicate that after internalization of Nap₂₀-HSA the conjugate is proteolytically degraded leading to the formation of the lysine conjugate of Nap. This amino acid conjugate of Nap was shown in a previous study by us to be equipotent to Nap itself with regard to prostaglandin-E₂ synthesis inhibition. A pronounced altered intrahepatic distribution was observed when Nap was coupled to lactosaminated and mannosylated HSA (Lact-HSA and Man-HSA, respectively). Coupling of Nap to Lact₇-HSA and Man₁₀-HSA resulted in a major shift in intrahepatic distribution from endothelial cells to the hepatocytes and Kupffer cells, respectively. We conclude that conjugation of Nap to HSA itself results in a selective delivery to endothelial cells and that the local proteolysis of the conjugate produces an active catabolite. Selective delivery to other cell types of the liver can be achieved by attaching naproxen to neoglycoproteins with an appropriate type and number of sugar groups.

Site-specific drug delivery can be achieved by linking drugs to various macromolecular carrier systems [1–3]. Such approaches that aim to increase local concentrations and simultaneously reduce unwanted side effects may both improve efficacy and safety of therapeutic agents. Selective delivery of pharmacologically active compounds to certain cell types in order to improve their metabolic function may also contribute to a better understanding of particular pathophysiological processes, residing in, or associated with, such cells.

Inflammation is a characteristic feature of various chronic diseases affecting different kinds of tissues and organs and can be treated with a large variety of drugs. Long term therapy with anti-inflammatory

agents, however, often coincides with various unwanted effects, like gastro-intestinal problems and/or kidney damage [4].

In many chronic liver diseases such as cirrhosis and fibrosis, inflammatory processes may play an important role. Gram-negative sepsis for instance induces secretion of various cytokines and eicosanoids mainly through the interaction of endotoxins with non-parenchymal cells of the liver [5, 6]. Various eicosanoids have been proposed to influence the course of such diseases. Some of these mediators may inhibit fibrotic and cirrhotic processes while others contribute to or sustain the development of these disorders [7]. The intercellular communication via such substances in the liver is considered to be a crucial mechanism in the development of pathology [6]. To restrict the side effects of various types of anti-inflammatory drugs in the therapy of liver

† Corresponding author: Tel. (31) 50-613215; FAX (31) 50-696619.

disease, site-specific drug delivery is an interesting option. Major side effects by such agents occur in the kidney [4]. By a covalent linkage to suitable carriers a more favorable distribution in the body might be achieved leading to an improved therapeutic index.

Neoglycoproteins have earlier been proposed to serve as carriers for various therapeutic agents to the liver [2, 3]. The hepatic clearance of these particular glycoproteins can be mediated by different types of receptors, depending on the exposed sugar and net charge of the molecule. Among others, galactose-recognizing receptors located at the surface of hepatocytes [8], two types of scavenger receptors present on endothelial cells and Kupffer cells, recognizing polymeric or monomeric negatively charged proteins, respectively [9], as well as glycoprotein receptors recognizing mannose residues on endothelial cells [10, 11] or mannose residues combined with negative charge on Kupffer cells [12] have been described. Binding of the (neo)-glycoproteins to these receptors is followed by endocytosis and most of the internalized material ends up in the lysosomes of the cells. In these organelles the proteins are digested into their single amino acid constituents. By linking drugs to such glycoproteins a cell specific delivery and subsequent liberation of pharmacologically active compound may in principle be achieved. In this respect, lactosaminated and mannosylated albumin have been proposed for targeting to hepatocytes and Kupffer cells, respectively [12, 13]. A potential problem in this targeting concept is that by coupling a number of drug molecules to the chosen glycoprotein carrier, the specific cellular recognition may be corrupted. Consequently an optimal compromise with regard to drug loading and maintenance of cell-specificity should be looked for [14, 15].

So far, this concept has been explored for various antineoplastic and antiviral agents [13, 16]. The present study was undertaken to examine this targeting modality for anti-inflammatory drugs. Naproxen (Nap[§]) was chosen as a model drug for the following reasons:

1. Naproxen has a relatively simple structure: the carboxyl group is the only reactive functional group and can be used for an amide linkage with the amino groups of proteins [17]. Carboxyl groups available for conjugation are present in many cyclo-oxygenase inhibitors as well as in some lipoxygenase inhibitors.

2. Nap and its metabolites can be analysed in biological material with highly sensitive and specific fluorimetric methods [17, 18].

3. The pharmacokinetics of Nap itself are well-known [19, 20].

In the present study Nap was covalently coupled to the following carrier proteins: human serum albumin (HSA), lactosaminated HSA (Lact₂₇-HSA) and mannosylated HSA (Man₁₀-HSA). The kinetics *in vivo* and in the isolated perfused rat liver were

studied. In addition, the intrahepatic cellular distribution and processing of the conjugates was examined. It is shown that in principle protein carriers can be designed to provide selective delivery of Nap-like compounds to the various cell types in the liver.

MATERIALS AND METHODS

Animals. Male Wistar rats (250–300 g) were fed a standard lab chow (Hope Farms N.V., Woerden, The Netherlands) and had free access to water.

Reagents and chemicals. Nap and HSA (fraction V) were obtained from the Sigma Chemical Co. (St Louis, MO, U.S.A.). The neoglycoproteins (Lact₂₇-HSA and Man₁₀-HSA) were synthesized by standard methods. Lactosamination was carried out by the method of Schwartz and Gray [21]; mannosylation was done by the procedure described by Kataoka and Tavassoli [22]. Succinylated HSA (Suc-HSA) was synthesized by the method of Jansen *et al.* [23]. ϵ -Nap-lysine was synthesized as described previously [17]. Acetonitrile and other reagents were of analytical or reagent grade. Water for HPLC analysis was of Millipore quality.

Synthesis and characterization of Nap-HSA, Nap-Lact₂₇-HSA and Nap-Man₁₀-HSA. Nap was coupled to HSA and the neoglycoproteins by the method of Franssen *et al.* [17] (Fig. 1). The degree of substitution was estimated by analysis of drug, protein content and number of unreacted amino groups of the protein as described before [17]. The total amount of covalently linked Nap was determined after alkaline hydrolysis of the different drug-protein conjugates. Briefly, 10 mg of the conjugate was treated with 1 mL 6 N NaOH. The solution was incubated at 80° for 72 hr. After acidification with 1.5 mL 6 N HCl, the hydrolysate was extracted with 6 mL dichloromethane. After evaporation of the organic solvent under a nitrogen atmosphere, the residue was dissolved in the HPLC eluent and the drug content was determined by HPLC. Non-covalently bound Nap was determined by direct extraction with dichloromethane. The amount of protein was determined according to Lowry *et al.* [24]. The number of free amino groups was established by the method of Habeeb [25].

Radioiodination. Proteins were labeled with ¹²⁵I to a specific activity of 0.1 μ Ci/ μ g by using a mild chloramine-T method [26]. Unattached ¹²⁵I was removed by gel filtration on a Sephadex G25 column. Immediately prior to the experiments non-covalently bound ¹²⁵I was removed on a PD-10 column and radioactivity recovered in the void volume was >98% precipitable with trichloroacetic acid which was added to a final concentration of 10%.

In the double-label experiments, proteins were labeled on both their tyrosine and lysine residues with ¹²⁵I and ¹³¹I, respectively. The tyrosine residues of Nap₂₀-HSA (0.1 μ Ci/ μ g) were labeled with ¹²⁵I using the chloramine-T method as described above [26]. The lysine residues of the conjugate were labeled with ¹³¹I via tyramine-cellobiose (TC) (1.0 μ Ci/ μ g) by the method of Hysing and Tolleshaug [27].

§ Abbreviations: HSA, human serum albumin; Nap, naproxen; Lact₂₇-HSA, lactosaminated HSA (27:1); Man₁₀-HSA, mannosylated HSA (10:1); Suc-HSA, succinylated human serum albumin; TC, tyramine-cellobiose.

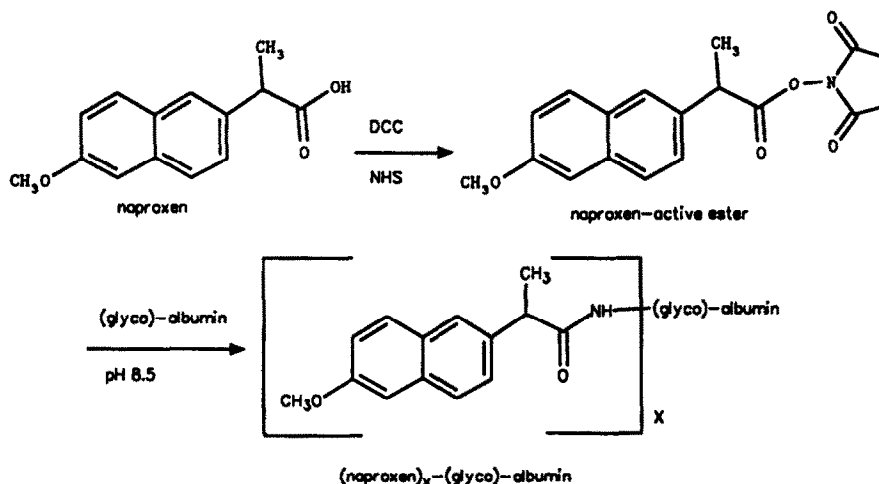


Fig. 1. Scheme for the preparation of Nap-albumin and the Nap-glycoalbumin conjugates. The x denotes variable degrees of drug substitution. DCC, dicyclohexylcarbodiimide; NHS, N -hydroxysuccinimide.

Fast Protein Liquid Chromatography (FPLC) characterization of the conjugates. Molecular mass estimation: The chromatographic behaviour on a Superose-12 column was studied to investigate whether the coupling reactions produced dimers or polymers as described previously [12]. In short, 100 μ L (1 mg/mL) of the conjugates was injected into the FPLC system equipped with a Superose-12 column (Pharmacia, Woerden, The Netherlands). Elution was performed with phosphate buffered saline, pH 7.4 at a flow rate of 0.5 mL/min.

Charge estimation: The relative net negative charge of the conjugates was determined on the FPLC system equipped with a Mono-Q anion exchange column (Pharmacia, Woerden, The Netherlands). Buffer A was a Tris-HCl buffer (0.02 M, pH 7.4) and buffer B was buffer A plus 1 M NaCl. Elution was performed at a flow rate of 0.25 mL/min with a gradient from 100% A to 100% B in 30 min. Again 100 μ L (1 mg/mL) of the conjugates was injected into the FPLC system.

Analysis of Nap and Nap-lysine. Nap and Nap-lysine were determined by HPLC with fluorescence detection by the method of Franssen *et al.* [18]. The mobile phase consisted of water-acetonitrile-acetic acid (60:40:1 by vol.); the flow rate was 2.0 mL/min. The column was a μ bondapak C-18 (Waters/Millipore Corp., Milford, MA, U.S.A.). The detector was a Waters 470 dual monochromator, operating at excitation wavelength 330 nm and emission wavelength 360 nm. Flurbiprofen was used as an internal standard, added prior to extraction and monitored simultaneously by UV-detection (Waters 440; 254 nm). Nap was determined after extraction. Briefly, plasma or tissue homogenates (100 μ L) were mixed with phosphate buffer 1 M pH 4.6 (freshly prepared containing 20 μ g/mL flurbiprofen), until a final volume of 2 mL; 6 mL of dichloromethane was added. The mixture was vortexed for 1 min and centrifuged at 3000 g for 10 min. The organic phase was evaporated under a

nitrogen atmosphere. The residue was dissolved in 300 μ L eluent and 100 μ L was injected into the HPLC. Nap in the form of covalently bound conjugates was analysed after alkaline hydrolysis of samples of plasma and tissue homogenates as described above. Nap-lysine was assayed by mixing plasma with two volumes of acetonitrile, centrifuged as described above and injected into the HPLC. Retention times were 3.1 min (Nap-lysine), 10.8 min (Nap) (mobile phase water-acetonitrile-acetic acid 60:40:1; flow 1.5 mL/min).

Qualitative analysis of ϵ -Nap-lysine in lysosomal preparation by LC-MS. The presence of ϵ -Nap-lysine was verified by the use of LC-MS with an ion-spray device by the method of Bruins *et al.* [28]. Chromatography conditions were similar as described above.

Immunohistochemical staining of liver sections. One milligram of the particular conjugate was injected in the vena penis dorsalis and after 10 min the animals were killed. Pieces of liver were immediately frozen in isopentane (-80°) and stored at -80° until sectioning. Sections of 4 μ m were cut in a cryostat (-20°). Staining of the endocytosed material and different cell types was performed as described previously by the method of Harms *et al.* [29].

Evaluation of intrahepatic distribution. The extent of uptake in different hepatic cell-types was evaluated by light microscopy. The content was graded semi-quantitatively on a 0-4+ scale (0 = absent; 1+ = low; 2+ = medium; 3+ = high; 4+ = very high).

Distribution of Nap₂₀-HSA in vivo. A bolus dose of the radioiodinated protein, Nap₂₀-[125 I- 131 I]TC-HSA (10 μ g and 5 mg), was injected into the vena penis dorsalis of anesthetized rats (pentobarbital, 60 mg/kg; i.p.) ($N = 4$ each). After 1 or 24 hr a blood sample was taken by heart puncture. After the animals were killed, the liver, kidneys, spleen, brain and plasma samples were counted in a LKB-Multichannel gamma counter for protein

measurement. For drug measurements similar experiments were carried out. Organs were removed and tissue homogenates were prepared as described before [30]. The weights of the organs were (\pm SD): the liver, 10.07 ± 2.24 ; the kidneys, 2.08 ± 0.18 ; the spleen, 0.66 ± 0.14 ; the brain, 1.39 ± 0.176 . The total volume of plasma was estimated to be 7.5 mL. Total amount of Nap and unconjugated Nap were assayed by HPLC as described above.

Isolated perfused rat liver experiments. Experiments with isolated perfused rat livers were performed as described previously [31]. Briefly, 12-hr fasted rats were anesthetized with pentobarbital (Nembutal® 60 mg/kg; i.p.). The bile duct, the portal vein and the superior vena cava were cannulated. The liver was excised and placed in the perfusion apparatus. The temperature was kept at 37°; the perfusate flow was maintained at 35 mL/min at a hydrostatic pressure of 10–12 cm. The recirculating perfusion medium (100 mL) consisted of a Krebs–bicarbonate buffer supplemented with 0.1% glucose and 1% bovine serum albumin and was constantly gassed with 95% oxygen and 5% carbon dioxide. To replace bile salts, an infusion of sodium taurocholate was given ($15 \mu\text{mol/hr}$). After a stabilization period of 20 min Nap- ^{125}I -HSA (0.5, 25, 100, 300, 400 μg , $N = 3$) was injected into the mixing chamber and, at the indicated times, perfusate samples of 300 μL were taken and mixed with 300 μL ice-cold 20% trichloroacetic acid. These mixtures were vortexed and centrifuged at 2500 rpm for 10 min. The pellets were washed with 600 μL trichloroacetic acid 20%. The radioactivity of the combined supernatant and pellet was counted in a LKB-Multichannel gamma counter. In the competition experiments, 25 mg Suc-HSA was given 5 min prior to injection of Nap- ^{125}I -HSA.

Drug release of Nap $_{20}$ -HSA after incubation with lysosomal lysates of the liver. Triton WR-1339-filled

lysosomes were prepared by the method of Huisman *et al.* [32]. The lysosomal fraction was purified 50 ± 12 -fold (mean \pm SD; nine isolations) with respect to the homogenate as indicated by its specific acid phosphatase activity. Fractions were frozen in liquid nitrogen and stored at -20° . Before use in the incubation mixtures, they were diluted with an equal volume of distilled water and the lysosomal membranes were ruptured by three cycles of freezing in liquid nitrogen and thawing at 38°. Dipeptidase activities of these lysates were (nmol/min/mg protein): 31 (Ile-Glu); 14 (Ala-Leu); 21 (Glu-Ala); 46 (His-Leu) and 31 (Ile-Asp). In the catabolism studies, this lysosomal extract (20 μL) was diluted with 500 μL buffer (containing: HAc/NaAc 0.5 M, DTT 4 mM, 10 $\mu\text{g/mL}$ flurbiprofen; pH 5.0) and 250 μL conjugate solution [conjugates were freshly dissolved in water (Millipore quality)] and buffer was added until a final volume of 1.0 mL and a final concentration of 1.0 mg/mL. This solution was incubated at 37°. Samples (100 μL) were taken at indicated times and diluted with three volumes of methanol. The mixtures were vortexed and centrifuged (2 min, 3000 g) and stored at 4° until HPLC analysis. The supernatants (50 μL) were injected into the HPLC as described above.

Pharmacokinetic analysis. Kinetic studies were performed using the multifit modified CFT3 program [33], which was implemented on the Olivetti PC.

Statistical analysis. Statistical comparisons were made with Student's *t*-test after checking equality of variances with a *F*-test; $P < 0.05$ was selected as the minimal level of statistical significance.

RESULTS

Synthesis and characterization of the conjugates

Table 1 shows that by increasing the molar Nap to neoglycoprotein ratio in the reaction mixture, an

Table 1. Characterization of the conjugates

Drug conjugates	Nap:C	DS	RFAG	PC	MWc	CHc
Nap ₁ -HSA	1:1	0.98	61	90	NS	2.35
Nap ₅ -HSA	10:1	4.75	54	80	NS	3.73
Nap ₂₀ -HSA	100:1	20.15	12	68	NS	14.07
Nap ₄ -Man ₁₀ -HSA	50:1	3.98	17	56	NS	3.09
Nap ₅ -Lact ₂₇ -HSA	60:1	5.07	20	45	NS	5.91

Nap:C, the molar ratio of Nap versus the carrier (C) (HSA, Man₁₀-HSA and Lact₂₇-HSA) in reaction mixture.

DS, the degree of drug substitution: the number of Nap molecules per carrier molecule, as established by HPLC (Nap) and by analysis of protein content by the method of Lowry *et al.* [24].

RFAG, the number of residual free amino groups as established by the method of Habeeb [25].

PC, the protein content of the conjugate as established by the method of Lowry *et al.* [24], after lyophilization of the conjugates (% g/g).

MWc, the changes observed in molecular mass, as established by FPLC using a Superose-12 column. The values represent the shift in retention times as compared to the carrier itself (HSA, Man₁₀-HSA and Lact₂₇-HSA).

CHc, the changes observed in charge, as established by FPLC using the Mono-Q anion exchange column. The values represent the shift in retention times as compared to the carrier itself (HSA, Man₁₀-HSA and Lact₂₇-HSA).

NS, not significant.

enhanced amount of Nap was coupled to the protein as measured by HPLC. This coincided with a corresponding decrease in the number of unreacted amino groups of the albumin molecule (column RFAG). The increase in degree of drug substitution of the conjugates correlated with prolonged retention times as observed after elution on an anion exchange column (Fig. 2). This indicated enhanced net negative charges as compared to those of the unconjugated protein carriers (column CHc). As can be deduced from column MWc, the synthesis conditions were such that no polymeric products were obtained.

Distribution of Nap₂₀-HSA in vivo

The organ distribution of Nap₂₀-HSA was studied *in vivo* with respect to the disposition of both drug and protein. The fate of the drug was monitored by measuring total and free amount of drug. The fate of the protein was monitored by a double labeling technique. This technique allowed discrimination between initial uptake and uptake followed by degradation. The results, expressed as absolute values (% dose/g tissue) and relative values (liver to kidney ratios), are shown in Tables 2–6. All values in Tables 2–5 are expressed as the % dose/organ

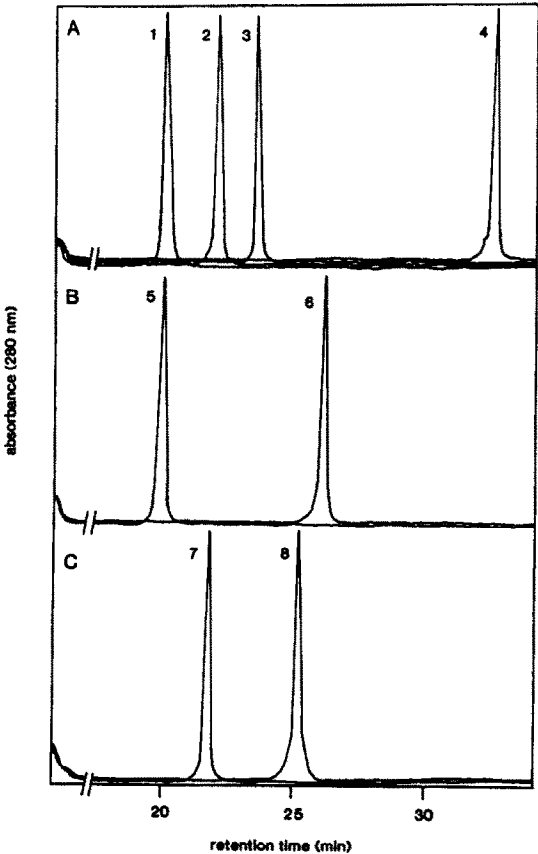


Fig. 2. FPLC-characterization of Nap_x-HSA (A), Nap_x-Lact₂₇-HSA (B) and Nap_x-Man₁₀-HSA (C). The retention time on the Mono-Q anion exchange column is related to the net negative charge. 1, HSA; 2, Nap₁-HSA; 3, Nap₅-HSA; 4, Nap₂₀-HSA; 5, Lact₂₇-HSA; 6, Nap₅-Lact₂₇-HSA; 7, Man₁₀-HSA and 8, Nap₄-Man₁₀-HSA.

Table 2. Protein and drug disposition of 10 µg HSA and 400 ng Nap as measured 1 hr after administration, injected in the form of a mixture (Nap + HSA), the conjugate Nap₂₀-HSA or as a single dose*

Compound	Liver	Kidneys	Spleen	Brain	Plasma
[¹²⁵ I]TC					
Nap ₂₀ -HSA	55.1 ± 0.28 (5.47)	0.8 ± 0.03 (0.38)	1.6 ± 0.18 (2.43)	0.01 ± 0.003 (0.007)	3.7 ± 0.82 (0.49)
HSA (single)	9.5 ± 0.34 (0.94)	2.03 ± 0.064 (0.976)	0.545 ± 0.0052 (0.828)	0.052 ± 0.0092 (0.037)	42.7 ± 0.34 (5.69)
Nap + HSA	8.3 ± 0.29 (0.82)	1.2 ± 0.11 (0.58)	0.5 ± 0.12 (0.76)	0.050 ± 0.0093 (0.036)	44.5 ± 0.98 (5.93)
[¹²⁵ I]					
Nap ₂₀ -HSA	58.5 ± 0.45 (5.80)	6.45 ± 0.059 (3.10)	3.0 ± 0.13 (4.56)	0.16 ± 0.011 (0.12)	19.2 ± 0.33 (2.56)
HSA (single)	3.4 ± 0.38 (0.34)	1.29 ± 0.099 (0.620)	0.25 ± 0.053 (0.38)	0.049 ± 0.0055 (0.035)	28.8 ± 0.94 (3.84)
Nap + HSA	3.3 ± 0.44 (0.33)	1.01 ± 0.094 (0.48)	0.25 ± 0.028 (0.38)	0.048 ± 0.0066 (0.034)	29.2 ± 0.88 (3.89)

* The values are expressed as the % dose/organ (mean ± SD, N = 4). The values between brackets denote % dose/g organ.

Table 3. Protein and drug disposition of 10 µg HSA and 400 ng Nap as measured 24 hr after administration, injected in the form of a mixture (Nap + HSA), the conjugate Nap₂₀-HSA or as a single dose*

Compound	Liver	Kidneys	Spleen	Brain	Plasma
[¹²⁵ I]TC					
Nap ₂₀ -HSA	17.0 ± 0.33 (1.69)	0.28 ± 0.038 (0.137)	0.66 ± 0.043 (1.00)	0.008 ± 0.0033 (0.006)	0.53 ± 0.076 (0.071)
HSA (single)	14.3 ± 0.88 (1.42)	1.46 ± 0.082 (0.702)	1.38 ± 0.085 (2.10)	0.025 ± 0.0099 (0.018)	8.57 ± 0.062 (1.14)
Nap + HSA	13.8 ± 0.79 (1.37)	1.39 ± 0.033 (0.668)	1.32 ± 0.039 (2.01)	0.024 ± 0.0077 (0.017)	8.49 ± 0.092 (1.13)
[¹²⁵ I]					
Nap ₂₀ -HSA	1.71 ± 0.061 (0.17)	1.24 ± 0.030 (0.596)	0.071 ± 0.0041 (0.108)	0.0035 ± 0.000510 (0.0025)	0.0003 ± 0.00018 (0.0004)
HSA (single)	1.18 ± 0.088 (0.12)	0.31 ± 0.078 (0.15)	0.118 ± 0.0022 (0.179)	0.018 ± 0.0035 (0.013)	6.52 ± 0.085 (0.869)
Nap + HSA	1.16 ± 0.053 (0.12)	0.29 ± 0.029 (0.14)	0.116 ± 0.0034 (0.176)	0.018 ± 0.0036 (0.013)	6.48 ± 0.084 (0.864)

* The values are expressed as the % dose/organ (mean ± SD, N = 4). The values between brackets denote % dose/g organ.

Table 4. Protein and drug disposition of 5 mg HSA and 200 µg Nap as measured 1 hr after administration, injected in the form of a mixture (Nap + HSA), the conjugate Nap₂₀-HSA or as a single dose*

Compound	Liver	Kidneys	Spleen	Brain	Plasma
[¹²⁵ I]TC					
Nap ₂₀ -HSA	26.7 ± 0.84 (2.65)	1.1 ± 0.12 (0.53)	1.3 ± 0.15 (1.98)	0.11 ± 0.012 (0.07)	27.9 ± 0.99 (3.72)
HSA (single)	9.0 ± 0.86 (0.89)	2.1 ± 0.34 (1.01)	0.5 ± 0.11 (0.76)	0.20 ± 0.045 (0.14)	70.7 ± 0.88 (9.43)
Nap + HSA	6.5 ± 0.33 (0.65)	1.4 ± 0.33 (0.67)	0.3 ± 0.18 (0.46)	0.05 ± 0.012 (0.04)	52.4 ± 0.79 (6.99)
[¹²⁵ I]					
Nap ₂₀ -HSA	31.7 ± 0.66 (3.15)	7.0 ± 0.44 (3.37)	1.8 ± 0.71 (2.74)	1.15 ± 0.031 (0.83)	6 ± 1.0 (0.8)
HSA (single)	4.3 ± 0.19 (0.43)	2.0 ± 0.11 (0.96)	0.35 ± 0.021 (0.35)	0.20 ± 0.019 (0.14)	73 ± 1.4 (9.73)
Nap + HSA	2.4 ± 0.23 (0.24)	1.35 ± 0.072 (0.65)	0.21 ± 0.041 (0.30)	0.05 ± 0.032 (0.04)	54 ± 1.2 (7.27)
Nap					
Nap ₂₀ -HSA	12.7 ± 0.16† (1.26)	0.58 ± 0.020 (0.28)	0.64 ± 0.022 (0.96)	<0.014 (<0.01)	28.9 ± 0.59‡ (3.85)
HSA (single)	4.13 ± 0.044 (0.41)	0.87 ± 0.070 (0.42)	0.26 ± 0.018 (0.40)	0.08 ± 0.012 (0.06)	25.4 ± 0.58 (3.38)
Nap + HSA	4.23 ± 0.052 (0.42)	0.98 ± 0.069 (0.47)	0.22 ± 0.016 (0.33)	0.08 ± 0.011 (0.06)	24.4 ± 0.73 (3.25)

* The values are expressed as the % dose/organ (mean ± SD, N = 4). The values between brackets denote % dose/g organ.

† 32% was recovered in the form of Nap-lysine and 2% in the form of free Nap.

‡ 4% (0.16% dose/mL) was recovered in the form of Nap-lysine and <1% in the form of free Nap.

Table 5. Protein and drug disposition of 5 mg HSA and 200 µg naproxen as measured 24 hr after administration, injected in the form of a mixture (Nap + HSA), the conjugate Nap₂₀-HSA or as a single dose*

Compound	Liver	Kidneys	Spleen	Brain	Plasma
[¹³¹ I]TC					
Nap ₂₀ -HSA	53.8 ± 0.92 (5.34)	0.7 ± 0.10 (0.34)	2.0 ± 0.12 (3.04)	<0.01 (<0.007)	1.45 ± 0.036 (0.19)
HSA (single)	17.3 ± 0.66 (1.72)	1.75 ± 0.077 (0.84)	1.55 ± 0.090 (2.36)	<0.01 (<0.007)	12.3 ± 0.63 (1.65)
Nap + HSA	15.7 ± 0.79 (1.56)	1.75 ± 0.053 (0.84)	1.2 ± 0.10 (1.82)	<0.01 (<0.007)	11.0 ± 0.73 (1.46)
¹²⁵ I					
Nap ₂₀ -HSA	1.2 ± 0.11 (0.12)	0.4 ± 0.09 (0.19)	<0.01 (<0.02)	<0.01 (<0.007)	0.15 ± 0.067 (0.02)
HSA (single)	1.5 ± 0.17 (0.15)	0.5 ± 0.08 (0.24)	0.15 ± 0.032 (0.23)	<0.01 (<0.007)	14 ± 2.0 (1.87)
Nap + HSA	1.65 ± 0.18 (0.16)	0.5 ± 0.07 (0.24)	0.15 ± 0.023 (0.23)	<0.01 (<0.007)	13 ± 1.8 (1.73)
Nap					
Nap ₂₀ -HSA	1.52 ± 0.046† (0.15)	0.166 ± 0.032 (0.08)	0.072 ± 0.0020 (0.11)	<0.01 (<0.001)	5.44 ± 0.073‡ (0.725)

* The values are expressed as the % dose/organ (mean ± SD, N = 4). The values between brackets denote % dose/g organ.

† 82% was recovered in the form of Nap-lysine and 13% in the form of free Nap.

‡ 90% (0.7% dose/mL) was recovered in the form of Nap-lysine and <1% in the form of free Nap.

Table 6. Tissue selectivity* of Nap₂₀-HSA

Compound	1 hr after injection			24 hr after injection		
	[¹³¹ I]TC	¹²⁵ I	Nap	[¹³¹ I]TC	¹²⁵ I	Nap
10 µg protein and 400 ng Nap						
Nap ₂₀ -HSA	14.4	1.87	—	12.3	0.29	—
HSA (single dose)	0.96	0.55	—	2.0	0.8	—
Nap + HSA	1.4	0.69	—	2.1	0.9	—
5 mg protein and 200 µg Nap						
Nap ₂₀ -HSA	5.0	0.9	4.5	15.7	0.63	1.9
HSA (single dose)	0.9	0.45	—	2.0	0.67	—
Nap (single dose)	—	—	0.98	—	—	—
Nap + HSA	0.97	0.37	0.89	1.9	0.67	—

* Tissue selectivity is expressed as the liver to kidney ratio (L/K), calculated as the ratio of the individual values (% dose/g tissue). These calculated values are based on protein measurement, as established by radioiodination ([¹³¹I]TC and ¹²⁵I) and total Nap measurement, as established by HPLC (Nap) [mean values (N = 4)].

(mean \pm SD, $N = 4$). The values between brackets denote % dose/g organ.

The influence of covalent drug incorporation with respect to disposition of both protein and drug was studied with the liver to kidney ratio (L/K) as a parameter for their disposition selectivity. One hour after injection, the L/K-protein-[^{131}I]TC values were significantly increased after injection of both 10 μg and 5 mg Nap₂₀-HSA: 15.0-fold (conjugation) vs 1.4-fold (mixture) and 5.6-fold (conjugation) vs 1.1-fold (mixture), respectively. The L/K-protein- ^{125}I values were also increased (3.4 vs 1.2 and 2.0 vs 0.8, respectively). This coincided with an increase of the L/K-Nap concentration ratio: 4.6 (conjugation) vs 0.9 (mixture) (in the case of the 5 mg dose). Similar results were found 24 hr after injection. These data clearly indicated a major and initial hepatic selectivity of both protein and drug by the covalent binding to albumin *per se*.

Cellular distribution of the conjugates

Table 7 shows the uptake of the conjugates in different liver cell types. Nap₂₀-HSA was mainly located in the endothelial cells. Nap-Lact₂₇-HSA was predominantly taken up in hepatocytes and Nap-Man₁₀-HSA was selectively taken up by Kupffer cells. The last two conjugates also showed some distribution to endothelial cells.

Experiments in the isolated perfused rat livers

The mechanism and characteristics of the selective hepatic distribution were further investigated in isolated perfused rat livers. The perfusate disappearance of 0.5 μg Nap₂₀-HSA is shown in Fig. 3.

Nap₂₀-HSA was removed from the perfusate with an initial half life of 5.5 min. The corresponding clearance was 12.7 mL/min. After a lag-time of approximately 10 min, trichloroacetic acid soluble

Table 7. Intercellular hepatic distribution of the carriers and their Nap conjugates

Compound	Cell-type		
	PC	KC	EC
HSA	0	0	0
Lact ₂₇ -HSA	++++	0	0
Man ₁₀ -HSA	0	++++	0
Suc-HSA	0	+	+++
Nap ₁ -HSA	0	0	+
Nap ₅ -HSA	0	0	++
Nap ₂₀ -HSA	0	+	+++
Nap ₅ -Lact ₂₇ -HSA	+++	0	+
Nap ₄ -Man ₁₀ -HSA	0	+++	+

PC, parenchymal cells; KC, Kupffer cells; EC, endothelial cells.

The content was graded semi-quantitatively by immuno-histochemical detection on a 0–4+ scale (0 = absent; 1+ = low; 2+ = medium; 3+ = high; 4+ = very high).

material, representing degraded material, started to appear in the perfusate. The total amount excreted in bile after 60 min was less than 0.5% of the dose. A V_{max} of 2.46 $\mu\text{g}/\text{min}$ per 10 g liver and a K_m of 4.27×10^{-6} M for the removal of Nap₂₀-HSA from the perfusate were established by kinetic analysis of the nonlinear decay curves [34].

The hepatic clearance could be inhibited by various polyanionic probes. Suc-HSA is a specific ligand for the scavenger receptor, located on endothelial cells [9]. Studies with this compound revealed that it inhibited liver uptake of Nap₂₀-HSA almost completely (Fig. 3). This suggests that scavenger receptors are of major importance in the removal of Nap₂₀-HSA by the liver.

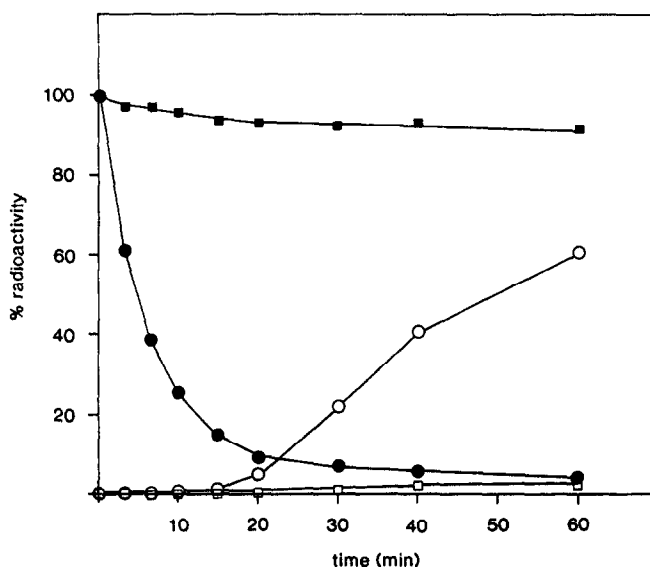


Fig. 3. Effects of 25 mg Suc-HSA (squares) on the perfusate disappearance of 500 ng of Nap₂₀-HSA in the isolated perfused liver. Circles denote controls. Acid-precipitable radioactivity is represented by closed symbols and open symbols refer to acid-soluble radioactivity. Data are means of three experiments.

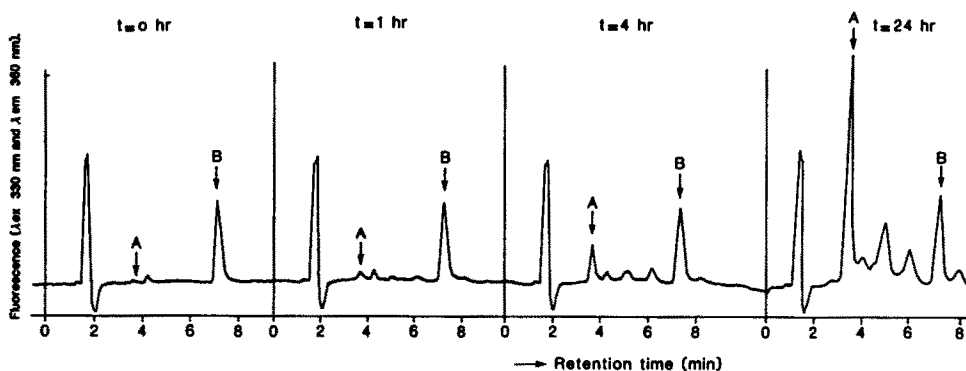


Fig. 4. HPLC after incubating Nap₂₀-HSA (1.0 mg/mL) with liver lysosomal lysates. Arrow A denotes Nap-lysine and arrow B denotes Nap.

Degradation of Nap₂₀-HSA by lysosomal lysates of the liver

The intracellular processing of Nap₂₀-HSA was further examined in lysosomal preparations (Fig. 4).

The main catabolite observed was ϵ -Nap-lysine ($M_r = 358$), as established by spiking known amounts of the pure compound to some of the samples and also by mass-spectral analysis. Control experiments with ϵ -Nap-lysine and Nap under similar conditions revealed that these compounds were not further metabolized. The rate of Nap-lysine formation was: 0.20 ± 0.035 nmol/mg/hr from Nap₂₀-HSA ($N = 3$), 1.61 ± 0.020 nmol/mg/hr from Nap-Lact₂₇-HSA ($N = 3$) and 0.49 ± 0.063 nmol/mg/hr from Nap-Man₁₀-HSA ($N = 3$).

DISCUSSION

The results presented in the present study demonstrate that hepatic delivery of drugs can be achieved *in vitro* by covalent coupling to native albumin *per se*. This was demonstrated by linking the anti-inflammatory drug Nap by its terminal carboxyl group to the lysine residues of native HSA. Only in case a covalent linkage was used, a selective distribution to the liver was obtained. As could be anticipated, non-covalent binding did not alter the disposition of the drug and protein significantly [30, 35]. Coupling to albumin seems an attractive option for drug delivery to endothelial cells of the liver. As anticipated, apart from the liver, elevated levels (albeit to a smaller extent) were also detected in the spleen, probably due to the presence of scavenger systems in the endothelial cells of this organ.

A completely different intrahepatic distribution was obtained by the introduction of specific sugar moieties in the albumin molecule. In this respect, galactose and mannose residues were shown to serve as homing devices for hepatocytes and Kupffer cells, respectively. These targeting strategies may be of use for a cell-specific delivery of prostaglandin and leucotriene synthesis inhibitors. Additionally, cell-specific delivery of such agents may provide cell-biological tools to study intercellular communication in the liver via various eicosanoids and thereby may

aid the elucidation of the complex pathophysiology of cirrhosis and fibrosis. So far, little is known about the specific uptake of such macromolecules in fat storing cells, cell types which are also involved in fibrogenetic pathophysiology [7].

Covalent coupling of the model drug Nap was done by an active ester activation. A major advantage of this coupling procedure above others is the absence of formation of polymeric and denaturated side-products [17]. The reaction resulted in formation of stable ϵ -amide bonds. This amide formation reduces the number of positively charged amino groups in the albumin molecule and thereby increases its net negative charge. In the present study this was confirmed by both analysis of free amino groups of the protein and anion exchange chromatography.

We reasoned that the enhanced negative charge of such drug-protein conjugates may promote binding to various scavenger receptors in the liver. These receptors have been established on endothelial cells [9, 36–38] and Kupffer cells [9, 34, 39]. Various polyanionic macromolecules like acetylated low density lipoproteins [40] and albumin [41] modified with anionic reagents were shown to bind avidly to these receptors followed by receptor-mediated endocytosis. Indeed our *in vivo* data clearly show the major involvement of the liver in the total clearance of Nap₂₀-HSA. The differences in the liver accumulation values between the two applied labels further indicate extensive catabolism into smaller peptide fragments *in vivo*. Since the [¹³¹I]Tc-label cannot escape from the intracellular space after protein digestion, the values calculated for this label reflect overall protein uptake [42, 43]. In contrast, the [¹²⁵I]-label can leave the cells in the form of free iodine or mono-iodotyrosine. Accumulation values based on this label therefore result from the combination of uptake and degradation of the protein. The corresponding accumulation value as measured in the organs for total Nap confirmed the enhanced hepatic uptake of this drug through coupling to the albumin. These data further indicate an intracellular release and partial efflux of Nap from the cells, mainly in the form of its amino acid conjugate Nap-lysine.

In the experiments with the isolated perfused

livers we found direct evidence for a receptor-mediated uptake of the Nap conjugates. This uptake could be fully inhibited by various anionic probes like Suc-HSA. Furthermore, immunohistochemistry showed that the endothelial cells were the main sites of this uptake. Therefore we conclude that scavenger receptors located on the endothelial cells and recognizing proteins with an overall negative charge are mainly involved in the rapid hepatic clearance of Nap₂₀-HSA *in vivo*. Our findings seem to be in good agreement with those of others concerning albumins derivatized with anionic probes. For instance, a previous report about fluorescein-derivatized albumin also showed high hepatic clearances *in vitro* (10.0 mL/min vs 12.7 mL/min as measured for Nap₂₀-HSA) [15]. Studies with HSA conjugated with dinitrophenyl groups *in vivo* also showed rapid blood clearance. Skogh *et al.* [14] proposed hydrophobicity as a major determinant involved in this clearance. They showed that this blood clearance was independent of serum complement and was not affected by various sugars, like galactose and mannose. However, they did not investigate the influence of anionic or hydrophobic probes on the clearance.

Despite a major distribution of Nap₅-Lact₂₇-HSA to the hepatocytes, a small part of the conjugate was still recovered in the endothelial cells. A similar observation was made for Nap₄-Man₁₀-HSA. Like Man₁₀-HSA itself, Nap₄-Man₁₀-HSA was predominantly internalized by Kupffer cells. These liver macrophages are known to recognize specifically mannose residues combined with a negative charge [12]. The additional uptake in endothelial cells may indicate that the above mentioned scavenger receptor system, at least to some extent, contributes to the hepatic disposition of Nap₅-Lact₂₇-HSA and Nap₄-Man₁₀-HSA. At present it remains to be clarified whether, besides net charge, other characteristics such as size and hydrophobicity of the conjugates may affect the binding to these different types of receptors. In this respect, the nature of the drug, the linkage method as well as the degree of substitution may be critical determinants. This will be an interesting point for further investigation.

In drug targeting strategies with covalent drug-carrier complexes, one crucial condition to be fulfilled is the regeneration of the drug in an active form at the site of action [17, 44]. In the present study we have shown that this is the case for Nap conjugated to HSA and related neoglyco-albumins due to the biodegradability of the chosen carrier molecules. The experiments with the lysosomal preparations revealed that Nap was regenerated in the form of the active ϵ -Nap-lysine derivative. At this particular site this catabolite was not further converted into Nap itself. This finding parallels our earlier observation with Nap conjugated to lysozyme as a carrier for renal drug targeting [18]. In contrast to the major hepatic distribution for its albumin analog, this lysozyme drug-protein conjugate predominantly distributes to the kidneys as a result of glomerular filtration, followed by tubular reabsorption. Renal lysosomal digestion of this conjugate also resulted in formation of the Nap-lysine catabolite. Interestingly, this catabolite showed

equipotent activity *in vitro* with respect to cyclooxygenase inhibiting potency relative to that of the parent drug [18].

In conclusion, specific delivery of anti-inflammatory agents, like Nap, to endothelial cells of the liver is possible by their coupling to albumin *per se*. The enhanced negative charge and/or increased hydrophobicity introduced by coupling of up to 20 Nap molecules may promote binding to and uptake via scavenger receptors. Receptor-mediated endocytosis of these negatively charged monomeric conjugates in endothelial cells of the liver is likely since uptake could be largely inhibited by Suc-HSA. By attaching additional sugar moieties like galactose and mannose as homing devices for hepatocytes and Kupffer cells, respectively, a shift in distribution to these other cell-types was obtained. Local proteolysis of such drug conjugates in lysosomes may result in the formation of active catabolites, such as Nap-lysine, observed in the present study.

Acknowledgements—This study was financially supported by the Technical Foundation (STW) of the Dutch Organization for Scientific Research (NWO). The authors thank Dr Machiel Hardonk and Geert Harms for the performance of the immunohistochemical staining and evaluations and Ms A. van Zanten (Department of Nuclear Medicine) for performing the radioiodination of the proteins. Dr Joop Bouma (Department of Biochemistry) is acknowledged for the preparation of the lysosomal lysates.

REFERENCES

1. Poznansky MJ and Juliano RL, Biological approaches to the controlled delivery of drugs: a critical review. *Pharmacol Rev* 36: 277–336, 1984.
2. Meijer DKF, Molema G, Jansen RW and Moolenaar F, Design of cell-specific drug targeting preparations for the liver: where cell biology and medicinal chemistry meet. In: *Trends in Drug Research Proceedings of the Seventh Noordwijkerhout-Camerino Symposium, Noordwijkerhout, The Netherlands* (Eds. Timmerman H and Claassen V), pp. 303–332. Elsevier, Amsterdam, 1990.
3. Van der Sluijs P and Meijer DKF, Limitations on the specificity of targeting asialoglycoprotein–drug conjugates to hepatocytes. In: *Targeted Diagnosis and Therapy of Liver Diseases: Cell Surface Receptors and Liver-Directed Agents* (Eds. Wu GY and Wu CH), pp. 2352–26440. Marcel Dekker, New York, 1991.
4. Brune K and Beck WS, Towards safer nonsteroidal anti-inflammatory drugs. In: *Drugs in Inflammation*, pp. 13–25. Birkhauser, Basel, 1991.
5. Fox ES, Thomas P and Broitman SA, Hepatic mechanisms for clearance and detoxification of bacterial endotoxins. *J Nutr Biochem* 1: 620–628, 1990.
6. Castelijns E, Kuiper J, Van Rooij HCJ, Kamps JAAM, Koster JF and Van Berkel TJC, Endotoxins stimulate glycogenolysis in the liver by means of intercellular communication. *J Biol Chem* 263: 6953–6955, 1988.
7. Gressner AM, Liver fibrosis—perspectives in patho-biochemical research and clinical outlook. *Eur J Clin Chem Clin Biochem* 29: 293–311, 1991.
8. Ashwell G and Morell AG, The role of surface carbohydrates in the hepatic recognition and transport of glycoproteins. *Adv Enzymol* 41: 99–128, 1974.
9. Jansen RW, Molema G, Harms G, Kruijt JK, Van Berkel TJC, Hardonk MJ and Meijer DKF, Formaldehyde treated albumin contains monomeric

- and polymeric forms that are differently cleared by endothelial and Kupffer cells of the liver: evidence for scavenger receptor heterogeneity. *Biochem Biophys Res Commun* 180: 23–32, 1991.
10. Hubbard AL, Wilson G, Ashwell G and Stukenbrok H, An electron microscopic autoradiographic study of carbohydrate recognition systems in the rat liver. *J Cell Biol* 83: 47–64, 1979.
 11. Summerfield JA, Vergalla J and Jones A, Modulation of a glycoprotein recognition system on rat hepatic endothelial cells by glucose and diabetes mellitus. *J Clin Invest* 69: 1337–1347, 1982.
 12. Jansen RW, Molema G, Ching TL, Oosting R, Harms G, Moolenaar F, Hardonk MJ and Meijer DKF, Hepatic endocytosis of various types of mannose-terminated albumins. What is important, sugar recognition, net charge or the combination of these features. *J Biol Chem* 266: 3343–3348, 1991.
 13. Fiume L, Busi C, Mattioli A, Balboni PG and Barbanti-Brodano G, Hepatocyte targeting of adenine-9-beta-D-arabinofuranoside 5'-monophosphate (ara-AMP) coupled to lactosaminated albumin. *FEBS Lett* 129: 261–264, 1981.
 14. Skogh T, Stendahl O, Sundqvist T and Edebo L, Physicochemical properties and blood clearance of human serum albumin conjugated to different extents with dinitrophenyl groups. *Int Arch Allergy Appl Immunol* 70: 238–244, 1983.
 15. Van der Sluijs P, Bootsma HP, Postema B, Moolenaar F and Meijer DKF, Drug targeting to the liver with lactosylated albumins. Does the glycoprotein target the drug, or is the drug targeting the glycoprotein? *Hepatology* 6: 723–728, 1986.
 16. Molema G, Jansen RW, Pauwels R, De Clercq E and Meijer DKF, Targeting of antiviral drugs to T-4 lymphocytes. Anti-HIV activity of neoglycoprotein-AZTMP conjugates *in vitro*. *Biochem Pharmacol* 40: 2603–2610, 1990.
 17. Franssen EJF, Koiter J, Kuipers CAM, Bruins AP, Moolenaar F, De Zeeuw D, Kruizinga WH, Kellogg RM and Meijer DKF, Low molecular weight proteins as carriers for renal drug targeting. Preparation of drug-protein conjugates and drug-spacer derivatives and their catabolism in renal cortex homogenates and lysosomal lysates. *J Med Chem* 35: 1246–1259, 1992.
 18. Franssen EJF, Van Amsterdam RGM, Visser J, Moolenaar F, De Zeeuw D and Meijer DKF, Low molecular weight proteins as carriers for renal drug targeting: naproxen-lysozyme. *Pharm Res* 8: 1223–1230, 1991.
 19. Runkel R, Chaplin M, Boost G, Segre E and Forchielli E, Absorption, distribution, metabolism and excretion of naproxen in various laboratory animals and human subjects. *J Pharm Sci* 61: 703–708, 1972.
 20. Sugawara Y, Fuyihara M, Muira Y, Hayashida K and Takahashi T, Studies on the fate of naproxen. II Metabolic fate in various animals and man. *Chem Pharm Bull* 26: 3312–3321, 1978.
 21. Schwartz BA and Gray GR, Proteins containing reductively animated disaccharides: synthesis and characterization. *Arch Biochem Biophys* 181: 542–549, 1977.
 22. Kataoka M and Tavassoli M, A class of reagents for detection of sugar recognizing substances. *J Histochem Cytochem* 32: 1091–1094, 1984.
 23. Jansen RW, Molema G, Pauwels R, Schols D, De Clercq E and Meijer DKF, Potent *in vitro* anti-HIV-1 activity of modified human serum albumins. *Mol Pharmacol* 39: 818–823, 1991.
 24. Lowry OH, Rosebrough NJ, Farr AL and Randall RJ, Protein measurement with the Folin phenol reagent. *J Biol Chem* 193: 265–275, 1951.
 25. Habeeb AFSA, Determination of free amino groups in proteins by trinitrobenzenesulfonic acid. *Anal Biochem* 14: 328–336, 1966.
 26. Greenwood FC, Hunter WM and Glover JS, The preparation of ¹³¹I labeled human growth hormone or high specific activity. *Biochem J* 89: 114–123, 1963.
 27. Hysing J and Tolleshaug H, Quantitative aspects of the uptake and degradation of lysozyme in the rat kidney *in vivo*. *Biochim Biophys Acta* 887: 42–50, 1986.
 28. Bruins AP, Covey TR and Henion JD, Ion Spray Interface for combined liquid chromatography/atmospheric pressure ionization mass spectrometry. *Anal Chem* 59: 2642–2646, 1987.
 29. Harms G, Dijkstra CD, Lee YC and Hardonk MJ, Glycosyl receptors in macrophage subpopulations of rat spleen and lymph node. A comparative study using neoglycoproteins and monoclonal antibodies ED1, ED2 and ED3. *Cell Tissue Res* 262: 35–40, 1990.
 30. Frijlink HW, Franssen EJF, Eissens AC, Oosting R, Lerk CF and Meijer DKF, The effects of cyclodextrins on the disposition of intravenously injected drugs in the rat. *Pharm Res* 8: 380–384, 1991.
 31. Meijer DKF, Keulemans K and Mulder GJ, Isolated perfused rat liver technique. In: *Methods in Enzymology* (Ed. Jakoby WB), pp. 81–94. Academic Press, New York, 1981.
 32. Huisman W, Bouma JMW and Gruber M, Involvement of thiol enzymes in the lysosomal breakdown of native and denaturated proteins. *Biochim Biophys Acta* 297: 98–109, 1973.
 33. Scaf AHJ, Pharmacokinetic analysis with RUGFIT: an interactive pharmacokinetic computer program. *Biopharm Drug Dispos* 9: 415–446, 1988.
 34. Rowland M and Tozer TN, *Clinical Pharmacokinetics-Concepts and Applications*. Lea and Febiger, Philadelphia, 1989.
 35. Van der Sluijs P, Spanjer HH and Meijer DKF, Hepatic disposition of cationic drugs bound to asialo-orosomucoid: lack of co-endocytosis and evidence for intrahepatic dissociation. *J Pharmacol Exp Ther* 240: 668–673, 1987.
 36. Pitas RE, Boyles J and Mahley RW, Uptake of chemically modified low density lipoproteins *in vivo* is mediated by specific endothelial cells. *J Cell Biol* 100: 103–117, 1985.
 37. Blomhoff R, Drevon CA, Eskild W, Helgerud P, Norum KR and Berg T, Clearance of acetyl low density lipoprotein by rat liver endothelial cells. *J Biol Chem* 259: 8898–8903, 1984.
 38. Eskild W and Berg T, High sensitivity towards monensin of receptor mediated endocytosis of formaldehyde treated human serum albumin by liver endothelial cells. *Biochim Biophys Acta* 968: 143–150, 1988.
 39. Buys CHCM, Elferink MGL, Bouma JMW, Gruber M and Nieuwenhuis P, Proteolysis of formaldehyde-treated albumin in Kupffer cells and its inhibition by suramin. *J Reticuloendothel Soc* 14: 209–223, 1973.
 40. Nagelkerke JF, Barto KP and Van Berkel TJC, *In vivo* and *in vitro* uptake and degradation of acetylated low density lipoprotein by rat liver and endothelial, Kupffer and parenchymal cells. *J Biol Chem* 258: 12221–12227, 1983.
 41. Haberland ME and Fogelman AM, Scavenger receptor mediated recognition of maleyl bovine plasma albumin and the demaleylated protein in human monocyte macrophages. *Proc Natl Acad Sci USA* 82: 2693–2697, 1985.
 42. Pittman RC, Carew TE, Glass CK, Green SR, Taylor CA and Attie AD, A radioiodinated, intracellularly trapped ligand for determining the sites of plasma protein degradation *in vivo*. *Biochem J* 212: 791–800, 1983.
 43. Hysing J, Tolleshaug H and Curthoys NP, Reabsorption

- and intracellular transport of cytochrome *c* and lysozyme in rat kidney. *Acta Physiol Scand* **140**: 419–427, 1990.
44. Trouet A, Masquelier M, Baurain R and Deprez-De Campeneere D, A covalent linkage between daunorubicin and proteins that is stable in serum and reversible by lysosomal hydrolysis as required for a lysosomotropic drug-carrier conjugate: *in vitro* and *in vivo* studies. *Proc Natl Acad Sci USA* **79**: 626–629, 1982.